A Comprehensive Review on Microstrip Couplers: Structure, Design Method, and Performance

Abbas Rezaei[1], Salah I. Yahya[2,3], and Leila Nouri[4,5]

[1]Department of Electrical Engineering, Kermanshah University of Technology,
Kermanshah, Iran

[2]Department of Communication and Computer Engineering, Cihan University-Erbil,
Erbil, Iraq

[3]Department of Software Engineering, Faculty of Engineering, Koya University,
Koya KOY45, Iraq

[4]Institute of Research and Development, Duy Tan University,
Da Nang 550000, Vietnam

[5]Faculty of Electrical – Electronic Engineering, Duy Tan University,
Da Nang 550000, Vietnam

Abstract—In this paper, several types of microstrip couplers are investigated in terms of structure, performance, and design methods. These planar 4-ports passive devices transmit a signal through two different channels. Designers' competition has always been in miniaturizing and improving performance of couplers. Proposing a novel structure is an advantage of some previously reported couplers. A high-performance coupler should have high isolation and low losses at both channels. The common port return loss in the pass band should have a low value. Among the couplers, those with balanced amplitude and phase are more popular. The popular mathematical analysis methods are even/odd mode analysis, extracting the information from the ABCD matrix and analyzing the equivalent *LC* circuit of a simple resonator. According to the phase shift value, couplers are classified as 90º and correct multiples of 90º, where a microstrip 0º coupler can be used as a power divider. Some couplers have filtering and harmonic elimination features that are superior to other couplers. However, few designers paid attention to suppressing the harmonics. If the operating frequency is set in according to the type of application, the coupler becomes particularly valuable.

Index Terms—ABCD matrix, Branch-line, Coupler, Directional, Microstrip

I. Introduction

In classification, microstrip couplers can be divided into two main categories: branch-line and directional couplers. The other types of couplers are ring couplers, rate race couplers, etc., which have been less reported. Microstrip branch-line couplers (BLCs) are a type of quadrature hybrid. Many BLCs, Ring and rat-race couplers, have been reported using different microstrip structures. In (Chi, et al., 2012) interdigital radial cells (ring structure), in (Salehi, Noori and Abiri, 2015; Salehi and Noori, 2014; Rezaei, Noori and Hosseini, 2018) high/low impedance sections (branch-line structures), in (Sun, et al., 2005) discontinuous microstrip lines, in (Lai and Ma, 2013) interdigital series structures (rat-race structure), in (Tian, et al., 2019) composite planar transmission lines, and in (Maheswari and Jayanthy, 2022) a simple hollow rectangle is utilized to obtain the microstrip couplers. To miniaturize, the simple conventional rectangle of the branch-line coupler is loaded by T-shape inner stubs in (Lalbakhsh, et al., 2021). By bending the transmission lines in a compact space (instead of the conventional rectangle) a new multi-channel branch-line coupler is designed in (Tang and Chen, 2009). A 3-dB BLC is introduced in (Abouelnaga and Mohra, 2017) with good isolation and large negative common port return loss in dB. However, it has not a filtering frequency response. To achieve the bandpass filtering couplers, coupled lines are a good choice which have been used in (Nie, et al., 2019; Arriola, Lee and Kim, 2021; Noori and Rezaei, 2018; Shi, et al., 2016). To suppress the harmonics, the couplers with low-pass filtering frequency responses are designed in (Khan, Mehdi and Zhao, 2019; Roshani, et al., 2022; Kim and Kong, 2010). Two series rectangles (2-section) in (Shukor and Seman, 2016; Mojarrad and Basharat, 2015) and four series rectangles (4-section) in (Tang, et al., 2006) are used to design BLCs. Interestingly, where two rectangles are in series, there are two transmission poles (TPs) (Shukor and Seman, 2016; Mojarrad and Basharat, 2015) and where four

rectangles become series, four TPs have been created in the passband (Tang, et al., 2006). Similarly, several rectangular loops (multi-section) have been integrated in series to create several TPs in the bandpass in (Tang, Tseng and Hsu, 2014), but it occupies a large area. To reach a novel structure, the conventional rectangle arms are carved in (Abdulbari, et al., 2021). For suppressing the harmonics up to the 14th, a new ring coupler is introduced in (Zhang and Zhang, 2019) which is a precious achievement. A 90□ hybrid coupler, with a large size, inspired by the structure of 2-section BLC is introduced in (Chiu, et al., 2014). A BLC with balanced magnitude and phase is indicated in (Velan and Kanagasabai, 2016) which is obtained by a little change in the proposed structure in (Tang and Chen, 2009). Triple-channel BLC with tunable operating frequencies is presented in (Liou, et al., 2009). A 3-dB BLC is designed in (Alhalabi, et al., 2018) to operate at 2.45 GHz for wireless local area networks (WLANs). Having very good isolation and return loss is two advantages of this work. Two 3-dB and 6-dB broadband BLCs working at 2 GHz with chebyshev frequency responses have been designed in (Smolarz, Wincza and Gruszczynski, 2020). Another 90º microstrip hybrid coupler with a wide fractional bandwidth (FBW) of 84.3% is presented in (Sun, et al., 2019) which has no isolation port. The fractional bandwidth of amplitude can be calculated using the upper and lower cutoff frequencies S_{21} and S_{31}. A BLC is designed in (Shukor and Seman, 2020) based on analyzing the substrate. This coupler works at 26 GHz which makes it suitable for fifth-generation (5G) applications. The other types of branch-line and rat-race couplers are designed in (Chen, Sim and Wu, 2016; Kao and Chen, 2000; Santiko, Saputera and Wahyu, 2016; Wang, et al., 2007; Shamsinejad, Soleimani and Komjani, 2018; Li, Qu and Xue, 2007).

Conventionally, a directional coupler comprises two parallel couple lines with four ports. A well-designed directional coupler should have high directivity, where, directivity is the ratio of forward power to reverse power. An ideal directional coupler will have an infinite value of directivity. To sample an RF signal passing in a microstrip transmission line the directional couplers are useful devices. It is utilized to couple the waves in one direction. They have been demanded by microwave circuits such as balanced mixers, antenna feeds and modulators (March, et al., 1982). A coupled-line capacitive-loaded directional coupler is designed in (Dydyk, et al., 1999). If a coupler structure is symmetric, the even/odd-mode phase velocities help to improve the isolation. According to this, a symmetric directional coupler using a pair of simple coupled lines similar to (Dydyk, et al., 1999) is proposed and analyzed (in terms of even/odd modes) in (Kim, et al., 2004). To realize a high directivity in (Kumar, et al., 2020), the structure of the conventional directional coupler is changed a little. Four coupled lines have been utilized in (Tripathi, et al., 2018) to improve the performance. The advantages of this coupler are a filtering frequency response with good directivity. Some directional couplers with high directivity have been reviewed in (Yaduvanshi and Bhatia, 2016) to show the main reason for poor performance. In (Kim, et al., 2001), the coupled parallel lines are bent in the middle and a u-shaped structure

is created to obtain a directional coupler with good isolation and directivity. In (Sanna, et al., 2018) a directional coupler with high isolation and tight coupling is proposed. Another directional coupler is designed by creating a bend in the coupled parallel lines in (Hong and Lancaster, 2001).

In this work, we will review several types of microstrip couplers in terms of branch-line couplers, directional couplers, ring couplers, etc. The size and substrate of some couplers will be reviewed. Moreover, we will investigate the various structures of couplers which lead to reach the different types of frequency responses. A perfect comparison of the couplers performance will be down. The comparison parameters are coupling factor, return loss, insertion loss, magnitude and phase balance, filtering response, and harmonics suppression. Furthermore, the operating frequency and applications of couplers will be studied. To compare the performance of directional couplers, directivity will also be added. A summary of the useful mathematical design methods is presented too.

II. Branch-Line, Ring, and Rat-Race Couplers

The layout of microstrip conventional branch-line coupler is presented in Fig. 1. This coupler works at 1 GHz which is suitable for GSM applications. As presented, it occupies a large implementation area. Designers of branch-line couplers are always competing to make this basic structure smaller. A Rogers_RT_Duroid 5880 with εr = 2.22 is used to simulate the conventional structure. The frequency response of this coupler for two different thicknesses of substrate layer is depicted in Fig. 1b and c, which is clear for h = 0.381 mm it has the better isolation (S_{41}) and common port return loss (S_{11}). Not having a filtering frequency response is one of the most important problems of this conventional structure. The bandpass filtering response is usually created using coupled lines. However, if a low-pass filter (LPF) structure is used on the conventional coupler arms, a low-pass filtering response will be produced and subsequently, the harmonics can be suppressed (Roshani, et al., 2022).

Some structures of the BLCs with their substrate properties and advantages are presented in Table I. As shown, the structures of couplers in (Rezaei, Noori and Hosseini, 2018; Tang and Chen, 2009; Roshani, et al., 2022) are novel. However, the complexity of the proposed structures in (Rezaei, Noori and Hosseini, 2018) and (Roshani, et al., 2022) leads to hard fabrication and subsequently, the possibility of manufacturing error will be high. Contrary to these structures, a very simple structure is proposed in (Maheswari and Jayanthy, 2022) In (Lalbakhsh, et al., 2021), six stubs were loaded inside a thin rectangular which led to create a low-pass filtering frequency response. The designed coupler in (Abouelnaga and Mohra, 2017) is built on a Teflon substrate. It has a relatively simple structure with good isolation and common port return loss. The structures reported in (Nie, et al., 2019) and (Khan, Mehdi and Zhao, 2019) are very similar and the dielectric constants in both structures are 2.2. This makes both of them able to suppress the harmonics. In (Arriola, Lee and Kim, 2021), the coupling used in the input/output ports leads to a filtering frequency
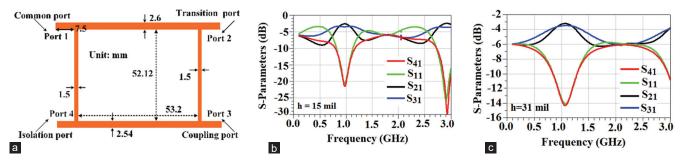
Fig. 1. Conventional branch-line coupler (a) layout of microstrip, (b) frequency response for $h = 0.381$ mm, and (c) frequency response for $h = 0.7874$ mm.

TABLE I
LAYOUT, SUBSTRATE AND ADVANTAGE OF SOME BLCS

References	Layout of BLCs	Substrate	ε_r	Thickness	Advantages
Rezaei, Noori and Hosseini, 2018		Rogers_RT_Duroid 5880	2.22	0.7874 mm	1. Low phase shift 2. Novel structure
Maheswari and Jayanthy, 2022		FR4	4.4	1.6 mm	1. Less design complexity and easy fabrication
Lalbakhsh, et al., 2021		RT/Duroid	2.2	0.508 mm	1. Balanced magnitude 2. Filtering frequency response 3. Suppressed harmonics
Tang and Chen, 2009		Rogers RO4003	3.38	0.508 mm	1. Novel structure 2. High isolation 3. Good common port return loss 4. Multipassband
Abouelnaga and Mohra, 2017		Teflon	2.2	0.7874 mm	1. High isolation 2. Good common port return loss
Nie, et al., 2019		---	2.2	0.508 mm	1. Filtering frequency response 2. Suppressed harmonics
Arriola, Lee and Kim, 2021		Chukoh	2.6	0.5 mm	1. Filtering frequency response 2. Wide passband
Khan, Mehdi and Zhao, 2019		F4BM-2	2.2	0.8 mm	1. Filtering frequency response 2. Suppressed harmonics
Roshani, et al., 2022		RT-Duroid	2.2	0.508 mm	1. Compact size 2. Novel structure 3. Filtering frequency response 4. Suppressed harmonics

BLCs: Branch-line couplers

response and subsequently the harmonics will be suppressed. As a result, the RT-Duroid substrate with $\varepsilon_r = 2.2$ is popular in designing the BLCs.

The frequency responses of some BLCs (presented in Table I) are shown in Figs. 2a-g, where the vertical and horizontal axes show S-parameters in dB and frequency in GHz, respectively. The operating frequency of the designed BLC in (Rezaei, Noori and Hosseini, 2018) is near 2.4GHz which is shown in Fig. 2a. Therefore, this coupler is appropriate for WLAN applications. Fig. 2b depicts an image of the scattering parameters in the narrow-band, while

in the wide-band view, the harmonics are well suppressed. Fig. 2c shows the multi-channel frequency response of the BLC designed in (Tang and Chen, 2009) whereas we can see the good values of return loss and isolation. As shown in Figs. 2d, e and g, the lowpass filtering frequency responses are obtained by (Nie, et al., 2019; Khan, Mehdi and Zhao, 2019; Roshani, et al., 2022). The relatively good values of isolation and return loss are indicated in the frequency response in (Abouelnaga and Mohra, 2017) (Fig. 3f).

The parameters of microstrip couplers can be calculated using the following formulas:
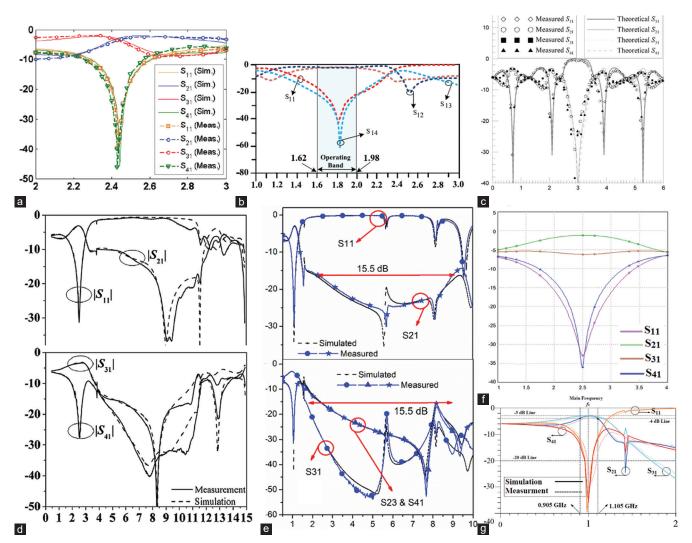
Fig. 2. Frequency response of some branch-line couplers in Table 1, (a) (Rezaei, Noori and Hosseini, 2018), (b) (Lalbakhsh, et al., 2021), (c) (Tang and Chen, 2009), (d) (Nie, et al., 2019), (e) (Khan, Mehdi and Zhao, 2019), (f) (Abouelnaga and Mohra, 2017), and (g) (Roshani, et al., 2022).

$$IL(dB) = -20\log(|S_{21}|)$$

$$RL(dB) = -20\log(|S_{11}|)$$

$$CF(dB) = -20\log(|S_{31}|) \quad (1)$$

$$I(dB) = -20\log(|S_{41}|)$$

Where IL, RL, CF, and I are insertion loss, common port return loss, coupling factor, and isolation respectively. However, we do not need to calculate these parameters. Because the EM simulator of Advanced Design System (and HFSS software) can give them to us from simulation results.

For designing most of BLCs mathematical theory, methods have been presented. Design methods sometimes include calculating the transfer matrix and extracting the necessary information from it (Salehi and Noori, 2014; Rezaei, Noori and Hosseini, 2018; Abouelnaga and Mohra, 2017; Nie, et al., 2019; Khan, Mehdi and Zhao, 2019; Kim and Kong, 2010; Smolarz, Wincza and Gruszczynski, 2020(. In some cases, the LC equivalent circuit of a small part of the couplers is presented and analyzed (Chi, et al., 2012; Rezaei, Noori and Hosseini, 2018; Sun, et al., 2005; Lai and Ma, 2013; Lalbakhsh, et al., 2021; Noori and Rezaei, 2018; Roshani,

et al., 2022; Abdulbari, et al., 2021; Chiu, et al., 2014; Liou, et al., 2009). Furthermore, even and odd modes have been analyzed for some symmetrical structures in (Abouelnaga and Mohra, 2017; Arriola, Lee and Kim, 2021; Tang, Tseng and Hsu, 2014; Sun, et al., 2019). In (Chi, et al., 2012), an equivalent LC circuit of a unit cell is proposed. Then unit-cell phase response is calculated using this LC circuit. In (Salehi, Noori and Abiri, 2015), even/odd modes analysis is done using the input impedance of a basic resonator. The analysis of the proposed BLC in (Salehi and Noori, 2014) is based on the ABCD matrix and the calculation of the reflection coefficient (Γ). It is important to note that we can extract, the insertion loss, return loss, and Γ from the ABCD matrix as follows (Salehi and Noori, 2014; Chen, et al., 2013):

$$IL = -20\log\left(\left|\frac{A + B/Z_0 - CZ_0 - D}{A + B/Z_0 + CZ_0 + D}\right|\right)$$

$$RL = -20\log\left(\left|\frac{2}{A + B/Z_0 + CZ_0 + D}\right|\right) \quad (2)$$

$$\Gamma = \frac{A + B - C - D}{A + B + C + D}$$

Where Z_0 is the impedance of terminals. The condition of having perfect impedance matching is obtained in (Rezaei, Noori and Hosseini, 2018), using ABCD matrix where $\Gamma = 1$. Under this condition the losses will be decreased significantly. Moreover, in (Rezaei, Noori and Hosseini, 2018), the resonance frequency is calculated under the perfect matching. In (Sun, et al., 2005), the phase velocity of a discontinuous transmission line is obtained based on an equivalent ladder LC circuit as follows:

$$v_p = \frac{1}{\sqrt{LC}} \qquad (3)$$

Where C and L are the inductance and capacitance of the ladder LC circuit. The analysis of BLC in (Lai and Ma, 2013) is based on finding the frequencies of transmission zeros. In (Maheswari and Jayanthy, 2022), the length of each arm (L_{arm}) is equal to λ/4, which is expressed as follows:

$$L_{arem} = \frac{\lambda}{4} = \frac{300}{4 f(GHz)\sqrt{\varepsilon_{re}}}$$

$$where: \varepsilon_{re} = \frac{1+\varepsilon_r}{2} + \frac{1-\varepsilon_r}{2}\left(\frac{1}{\sqrt{1+12h/w}}\right) \quad for: w/h \geq 1 \qquad (4)$$

In Equation (4), L_{arm} is in mm, w is the width of the arm in mm, and f is the frequency in GHz. Therefore, based on a predetermined target frequency and the value of the effective dielectric constant (ε_{re}), the length of each arm will be determined. The transfer function of an LC equivalent of a resonator in (Lalbakhsh, et al., 2021) is calculated. This LC circuit is a LPF that the authors calculated its cutoff frequency based on the values of lumped elements. In (Tang and Chen, 2009), the resonance frequencies of all passbands are calculated as some functions of the admittances of microstrip cells. To calculate the S-parameters in (Abouelnaga and Mohra, 2017), the even and odd modes ABCD matrices have been calculated, where the vector amplitudes of the signals emerging from the four ports are estimated as follows:

$$P_1 = 0.5(\Gamma_{Even} + \Gamma_{Odd})$$
$$P_2 = 0.5(T_{Even} + T_{Odd})$$
$$P_3 = 0.5(T_{Even} - T_{Odd})$$
$$P_4 = 0.5(\Gamma_{Even} - \Gamma_{Odd}) \qquad (5)$$

Where Γ and T are the reflection and transmission coefficients respectively. Moreover, the transmission parameters S_{21} and S_{31} are derived as follows:

$$S_{21} = 0.5(T_{Even} + T_{Odd})$$
$$S_{31} = 0.5(T_{Even} - T_{Odd}) \qquad (6)$$

The transition matrix of a quarter-wavelength transmission line, with an impedance of Z and 90º electrical length, is written in (Nie, et al., 2019) as follows:

$$M_{\lambda/4} = \begin{bmatrix} 0 & jZ \\ \frac{j}{Z} & 0 \end{bmatrix} \qquad (7)$$

The ABCD matrix in Equation (7) can be also used for the conventional branch-line coupler (Khan, Mehdi and Zhao, 2019). The ABCD matrix of a stub loaded transmission line presented in Fig. 3 is calculated as follows (Nie, et al., 2019):
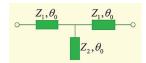
Fig. 3. Stub loaded transmission line where θ_0 is the electrical length.

$$M_{SLR} = \begin{bmatrix} Cos^2\theta_0 - Sin^2\theta_0(1+\frac{Z_1}{Z_2}) \\ jZ_1(2 Sin\theta_0 Cos\theta_0 - j\frac{Z_1^2}{Z_2} Sin^2\theta_0 \tan\theta_0) \\ \frac{j}{Z_1}2 Sin\theta_0 Cos\theta_0(1+\frac{Z_1}{Z_2}) \\ Cos^2\theta_0 - Sin^2\theta_0(1+\frac{Z_1}{Z_2}) \end{bmatrix} \qquad (8)$$

To match another transmission line to this stub-loaded line, the ABCD matrices of them should be equal. In (Shi, et al., 2016), for a coupling structure the coupling coefficients M_{12} and external quality factor are written as follows (Kumar, Tannous and Danshin, 1995):

$$M_{12} = \frac{Fractional\ Bandwidth}{\sqrt{g_1 g_2}}$$

$$Q_e = \frac{g_1 g_2}{Fractional\ Bandwidth} \qquad (9)$$

Where g-values are the lumped element values of the low-pass prototype filter with a cutoff frequency of 1 GHz. It should be noted that the coupler designed in (Shi, et al., 2016) has a bandpass filtering response so that we can define the external quality factor for it. In general, the quality factor is the ratio of the primary energy stored in the resonator to the energy lost in one radian of a oscillation cycle. For analyzing the proposed BLC in (Shukor and Seman, 2020; Chen, et al., 2013) the Q-factor due to the dielectric, Q_d is expressed as the following Equation:

$$Q_d = \frac{\varepsilon_{re}\sqrt{(\varepsilon_r - 1)}}{\varepsilon_r(\varepsilon_{re} - 1)\sqrt{\lambda_0} \tan\delta} \qquad (10)$$

Where λ_0 and tan δ are the wavelength in the air and the loss tangent, respectively. The value of ε_{re} can be calculated from Equation (4). Fig. 4 depicts the equivalent of the branch line with the ABCD matrix calculated in (Roshani, et al., 2022) as the following Equations:

$$T_{branch-line} = \begin{bmatrix} Cos2\theta_a - bSin2\theta_a \\ jZ_a(Sin2\theta_a - b(1-Cos2\theta_a)) \\ jY_a(Sin2\theta_a + b(1+Cos2\theta_a)) \\ Cos2\theta_a - bSin2\theta_a \end{bmatrix}$$

$$where:$$

$$b = \frac{Z_a}{2Z_b}(\tan\theta_{b1} + \tan\theta_{b2}) \qquad (11)$$

Since the ABCD-matrix of a quarter-wave line is written in Eq. (7), we can calculate the transition matrix of the conventional BLC, from Equation (10) as below (Kim and Kong, 2010):

$$T_{conventional} = \begin{bmatrix} 0 & jZ_a \tan\theta_a \\ jYa \cot\theta_a & 0 \end{bmatrix} \qquad (12)$$

The equivalent of a 2-section branch-line coupler is indicated in Fig. 5, where a, b, c, and d are the characteristic impedances of lines with electrical lengths of θ. From (Shukor and Seman, 2016; Kumar, Tannous and Danshin, 1995) we can write that:

$$a = d \frac{\sqrt{\frac{Z_{O2}}{Z_{O1}}\left(1 + \left|-j\frac{cd}{b^2}Z_{O1}\left(\frac{1}{a}+\frac{1}{d}-\frac{b^2}{abc}\right)\right|^2\right)} - 1}{\sqrt{\frac{Z_{O2}}{Z_{O1}}\left(1 + \left|-j\frac{cd}{b^2}Z_{O1}\left(\frac{1}{a}+\frac{1}{d}-\frac{b^2}{abc}\right)\right|^2\right)} - \frac{Z_{O2}}{Z_{O1}}} \qquad (13)$$

To show the advantages and disadvantages of the reported coupler, we compared them in Tables II and III. The return loss (RL), insertion loss (IL), coupling factor (CF), isolation (I), and phase imbalance (PI) of single-band couplers have been compared in Table II, where the RL, IL, CF, and I are best values of S_{11}, S_{21}, S_{31}, and S_{41} in dB inside the passbands. The summarized comparison results show that, the best values of RL, IL, CF, I, and PI are obtained in (Chi, et al., 2012; Rezaei, Noori and Hosseini, 2018; Tian, et al., 2019; Lalbakhsh, et al., 2021; Noori and Rezaei, 2018), respectively. Meanwhile, the most compact size is achieved in (Tian, et al., 2019) which is only 0.0044 λ_g^2, where λ_g is the calculated guided wavelength in the operating frequency in mm. The frequency response types, harmonic suppression, operating frequency (f_o), and applications of some single-band microstrip couplers are depicted in Table III. As written in Table III, the majority of them cannot suppress the harmonics. The best harmonic suppression is achieved in (Zhang and Zhang, 2019), where it could attenuate up to the 14th harmonic.
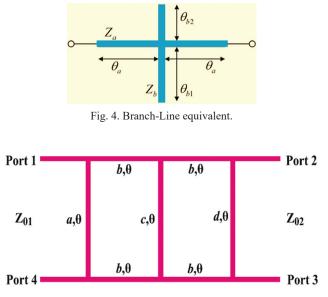

Fig. 4. Branch-Line equivalent.

Fig. 5. Equivalent of 2-section branch-line coupler.

III. Directional Couplers

A directional coupler may be composed of two parallel coupled lines with four ports. In the performance evaluation of directional couplers, in addition to the important parameters explained for other types of couplers, directivity parameter is important. This parameter is presented by D which can be calculated as $D = -20Log(/S23/)$ (Kim, et al., 2004). The layout structures, substrate features, and advantages of some directional couplers are presented in Table IV. The radial stubs have been used in (March, et al., 1982) to obtain a wide channel. The GaAs substrate with ε_r = 12.9, and h = 0.1 mm is used to design a simple directional coupler in (Kim, et al., 2004). Using a high dielectric constant will increase the normalized size. Therefore, in (Kim, et al., 2004), the value of the dielectric constant is decreased to 2.5. As written in Table IV, high directivity is achieved in (Tripathi, et al., 2018) and (Kim, et al., 2001) where high isolation is an achievement of (Kim, et al., 2004) and (Hong and Lancaster, 2001). Please note that the reported directional couplers are less than BLCs. The conventional directional coupler is presented in (Dydyk, et al., 1999).

Fig. 6 depicts the frequency response of the directional coupler in (Tripathi, et al., 2018), where they have been obtained for different values of the space between coupled lines. Based on this method, we can select the best values of the space between coupled lines. As shown in Fig. 6, by decreasing the space between coupled lines, the passband will be improved. Because, it leads to create two transition poles and reach the better value of insertion losses at the coupled and trough ports (S_{31} and S_{21}) whereas the best common port return loss is obtained under this condition. Since the coupling structure is an inseparable section from directional couplers, their frequency responses may be able to filter the undesired frequencies. Having a filtering response is a big advantage when harmonics are suppressed.

The performance and size of some directional couplers are compared in Table V. The reported coupler in (March, et al., 1982) works at 2.4 GHz for WLANs. Since the couplers in (Kim, et al., 2004) and (Tripathi, et al., 2018) work at 1.75 GHz and 1 GHz, they are suitable for GSM. Only, the introduced coupler in (Tripathi, et al., 2018) has a filtering frequency response, whereas it occupies a small area. The best values of directivity and isolation are obtained in (Kim, et al., 2001) and (Kim, et al., 2004), respectively. However, the proposed coupler in (Kim, et al., 2004) has an undesired coupling factor.

The number of rat race couplers is few. Therefore, it is not possible to draw a general conclusion about their phase behaviors. However, both rat race couplers given by (Lai and Ma, 2013) and (Lalbakhsh, et al., 2021) are 0º. It seems that the position of the output ports has an effect on this matter. Meanwhile, there are 0º (or 180º) and 90º (or 270º) branch-line couplers some couplers with asymmetric structures have been reported. The structures of the couplers presented in (Shi, et al., 2016), (Sun, et al., 2019) and (Kao and Chen, 2000) are asymmetric. Comparing the frequency response of these couplers shows that the symmetry or asymmetry does not have a significant effect on obtaining the filtering frequency response and the suppressing the harmonics. In general, it can

TABLE II
Comparison of single-band Microstrip Couplers in Terms of RL, I, PI and Size

Ref.	RL	S_{21} (dB)	S_{31} (dB)	I	PI	Size (λ_g^2)	Size (mm²)	FBW
Chi, et al., 2012	16.99	1.38	8.11	20.33	7.1º	---	---	---
Salehi, Noori and Abiri, 2015	18.2	3.1	3.1	19.3	0.8º	0.0425	55.8	---
Salehi and Noori, 2014	21.4	3.3	3.3	42.9	0.094º	0.023	175.12	---
Rezaei, Noori and Hosseini, 2018	29	3	3.08	30	0.037º	0.037	345.75	---
Sun, et al., 2005	35	---	---	35	0.5º	---	---	---
Lai and Ma, 2013	23.8	3.28	3.28	28.5	0.2º	0.0231	97.99	18.8%
Tian, et al., 2019	43.7	3.07	3.04	15	3.8º	0.00444	1600	---
Maheswari and Jayanthy, 2022	16.6	3.54	3.57	20.8	2.15º	0.285ª	560.7 ª	---
Lalbakhsh, et al., 2021	35	3.06	3.07	60	0.8º	0.0392	504.03	22%
Abouelnaga and Mohra, 2017	---	---	---	---	---	0.152ª	1161.37ª	---
Arriola, Lee and Kim, 2021	20	3.6±0.5	3.6±0.5	20	---	0.2379ª	1157.52	49%
Noori and Rezaei, 2018	29.5	3.3	2.8	31.3	0.97º	0.0754	534.36	---
Shi, et al., 2016	---	---	---	20	3º	0.138	---	3.5%
Khan, Mehdi and Zhao, 2019	29	3.5	3.02	29.7	2.1º	0.027	1287	30%
Roshani, et al., 2022	28	3	3	29	0.5º	0.008	428.49	20%
Kim and Kong, 2010	24	3.3	3.7	32	---	---	700	12.5%
Shukor and Seman, 2016	10	3±2	3±1.6	10	5º	---	1071.2	34.3%
Mojarrad and Basharat, 2015	20	3.25±0.1	3.25±0.1	20	1º	---	---	58%
Tang, et al., 2006	---	---	---	15	1º	---	---	40%
Tang, Tseng and Hsu, 2014	18.33	3.15	3.15±0.1	---	---	---	---	70%
Abdulbari, et al., 2021	30.69	2.97	3.65	29.28	3.6º	0.0432	432	30.22%
Zhang and Zhang, 2019	---	3.12	3.1	---	1.5º	0.039	630.12	24%
Chiu, et al., 2014	10	---	---	13	3º	---	4107	87%
Velan and Kanagasabai, 2016	19.43	3.49	3.68	22.98	0.08º	---	3584	37.8%
Liou, et al., 2009	15	---	---	15	5º	0.448	994.7	---
Alhalabi, et al., 2018	25.5	2.9	3.9	27.5	1º	---	338.3	---
Shukor and Seman, 2020	12	3±1	3±0.8	12	3º	0.307ª	595.01	---

ªWe calculate this using the information in the references. RL: Return loss, I: Isolation, PI: Phase imbalance, FBW: Fractional bandwidth

TABLE III
Comparison between BLCS in Terms of the Filtering Frequency Response, Harmonics, Operating Frequency and Applications

References	Filtering response	Frequency of the last attenuated harmonic	Nth suppressed harmonic	f_o (GHz)	Application
Chi, et al., 2012	Yes	No	No	2.4	WLANs
Salehi, Noori and Abiri, 2015	No	No	No	5.7	WLANs
Salehi and Noori, 2014	No	No	No	2.4	WLANs
Rezaei, Noori and Hosseini, 2018	No	No	No	2.4	WLANs
Sun, et al., 2005	No	No	No	1	GSM
Lai and Ma, 2013	Yes	7.2	3rd	2.4	WLANs
Tian, et al., 2019	No	No	No	0.5	Wireless Networks
Maheswari and Jayanthy, 2022	No	No	No	3.5	Wi-Max
Lalbakhsh, et al., 2021	Yes	12.6 GHz	7th	1.8	GSM
Abouelnaga and Mohra, 2017	No	No	No	2.5	Wireless Networks
Noori and Rezaei, 2018	Yes	15.1 GHz	5th	2.82	Wireless Networks
Shi, et al., 2016	Yes	2.3 GHz	1st	1.87	GSM
Khan, Mehdi and Zhao, 2019	Yes	10 GHz	9th	1	GSM
Roshani, et al., 2022	Yes	9 GHz	9th	1	GSM
Kim and Kong, 2010	Yes	2 GHz	2nd	1	GSM
Shukor and Seman, 2016	No	No	No	3.5	Wi-Max
Mojarrad and Basharat, 2015	No	No	No	2.4	WLANs
Tang, et al., 2006	No	No	No	2.4	WLANs
Tang, Tseng and Hsu, 2014	No	No	No	2.4	WLANs and Ultra-Wideband
Abdulbari, et al., 2021	No	No	No	3.55	Wi-Max and 5G
Zhang and Zhang, 2019	Yes	7 GHz	14th	0.5	Wireless Networks
Chiu, et al., 2014	No	No	No	1	GSM
Velan and Kanagasabai, 2016	No	No	No	0.433	Wireless Networks
Alhalabi, et al., 2018	No	No	No	2.45	WLANs
Smolarz, Wincza and Gruszczynski, 2020	No	No	No	2	Wireless Networks
Sun, et al., 2019	No	No	No	3	Wireless Networks

TABLE IV
Layout of Directional Couplers, Substrate Features and Their Advantages

Refs	Layout of BLCs	Substrate	ε_r	Thickness	Advantages
March, et al., 1982		Duroid	10.5	1.27 mm	1. Balanced phase 2. Wide channel
Dydyk, et al., 1999		GaAs	12.9	0.1 mm	1. Good RL
Kim, et al., 2004		---	2.5	0.7874 mm	1. High isolation
Tripathi, et al., 2018		FR-4	4.4	1.59 mm	1. High directivity 2. Filtering response 3. Novel structure
Kim, et al., 2001		---	---	---	1. High directivity 2. Novel structure
Hong and Lancaster, 2001		---	---	---	1. High isolation

BLCs: Branch-line couplers

TABLE V
Comparison among Previous Reported Directional Couplers

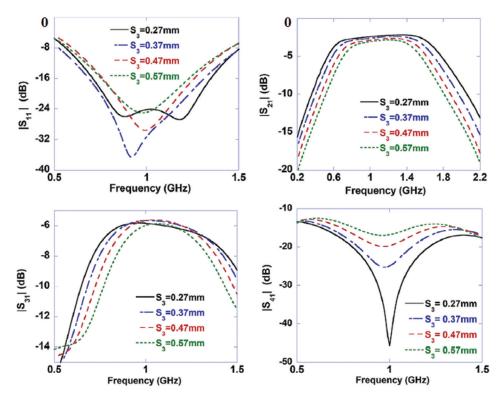| References	Return loss (dB)	S_{21} (dB)	S_{31} (dB)	Isolation (dB)	Directivity (dB)	f_o (GHz)	Filtering responses
March, et al., 1982	25	3.55±0.5	3.55	35	---	2.4	No
Kim, et al., 2004	---	---	20.2	47	26	1.75	No
Tripathi, et al., 2018	24.5	2.22	6.2	38	44	1.01	Yes
Kim, et al., 2001	---	---	3	---	68	2.5	No
Sanna, et al., 2018	30	---	3.15	30	32	2	No
Hong and Lancaster, 2001	---	5.8*	2.9	40	30	10.5	No

*Approximate value

Fig. 6. Scattering parameters of the directional coupler in (Tripathi, et al., 2018), where S_3 is the gap between two upper (and two lower) coupled lines.
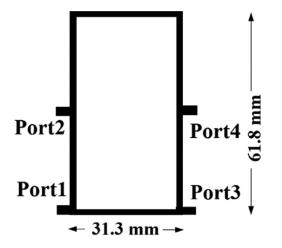
Fig. 7. The layout of conventional rat race coupler.

be said that the use of these asymmetric structures increases the size of some couplers. The conventional rat race coupler is depicted in Fig. 7. As shown in this figure, it occupies a large size of 1934.34 mm^2 (0.5 λg × 0.25 λg), where λg is the guided wavelength calculated at its 1.8 GHz operational frequency. The insertion losses of the conventional rat race couplers are <0.3 dB (Lalbakhsh, et al., 2021).

Three dual-band couplers are proposed by (Feng, et al., 2020), (Chang, et al., 2022) and (Jia, Zhang and Zhang, 2020) with the overall dimensions of 0.162 λg^2, 0.078 λg^2, and 0.156 λg^2, respectively. The dimensions of dual-band and multi-band couplers are usually larger than the dimensions of the single-band couplers. Designing multi-band couplers is much more difficult (Liou, et al., 2009). The multi-band coupler presented by (Liou, et al., 2009) occupies a large area of 0.448 λg^2 whereas it has a weak phase balance. The dual-band coupler designed by (Feng, et al., 2020) operates at 0.9/1.8 GHz which makes it suitable for GSM applications. The phase difference between two output ports of this coupler is 89.6º and 90.7º at the lower and upper channel, respectively, whereas these values for (Chang, et al., 2022) are 89.5º and 91.6º. The fractional bandwidths at the upper and lower channels of (Jia, Zhang and Zhang, 2020) are 34.7% and 14.9%, respectively. Two other special types of couplers are Lange and Bagley-polygon couplers. The Lange coupler is a four-port structure developed by Dr. Julius Lange in 1969. In order to design it, the interdigital cells have been used. Its structure is relatively similar to the coupler presented in (Tripathi, et al., 2018). Bagley-polygon couplers are another type of couplers that have a triangular structure, in which three ports are located on three vertices. Port 1 is located between ports 2, 3 on a side of the triangle. To achieve a better frequency response, the structure of this triangle can be optimized. As an example, we can change the width of the sides or load some blocks inside it.

IV. Conclusion

Several types of microstrip couplers including branch-lines, directional, rate-races, and rings are reviewed in this work. The structure, substrate, performance, advantages, and disadvantages of some of them were explained. The size and performance, in terms of insertion loss, return loss, coupling factor, isolation, directivity and phase balance, of these couplers are compared and reviewed. Moreover, the useful and popular mathematical design methods that presented in some reported works are investigated in this paper. We conclude that the even/odd mode analysis, extracting the main parameters from the ABCD matrix and analyzing the *LC* circuits are the favorite design methods.

References

Abdulbari, A.A., Rahim, S.K.A., Aziz, M.Z.A.A., Tan, K.G., Noordin, N.K., and Nor, M.Z.M., 2021. New design of wideband microstrip branch line coupler using T-shape and open stub for 5G application. *International Journal of Electrical and Computer Engineering*, 11(2), pp.1346-1355.

Abouelnaga, T.G., and Mohra, A.S., 2017. Reconfigurable 3 6 dB novel branch line coupler. *Open Journal of Antennas and Propagation*, 5, pp.7-22.

Alhalabi, H., Issa, H., Pistono, E., Kaddour, D., Podevin, F., Abouchahine, S., and Ferrari, P., 2018. Miniaturized branch-line coupler based on slow-wave microstrip lines. *International Journal of Microwave and Wireless Technologies*, 10(10), pp.1-4.

Arriola, W.A., Lee, J.Y., and Kim, I.S., 2021. Wideband 3 dB branch line coupler based on λ/4 open circuited coupled lines. *IEEE Microwave and Wireless Components Letters*, 21(9), pp.486-488.

Chang, H., Lim, T., Dimitrov, K.C., and Lee, Y., 2022. Dual-band branch-line coupler based on crossed lines for arbitrary power-split ratios. *Sensors*, 22, pp. 5527.

Chen, C.C., Sim, C.Y.D., and Wu, Y.J., 2016. Miniaturised dual-band rat-race coupler with harmonic suppression using synthetic transmission line. *Electronics Letters*, 52(21), pp.1784-1786.

Chen, C.F., Huang, T.Y., Shen, T.M., and Wu, R.B., 2013. Design of miniaturized filtering power dividers for system-in-a-package. *IEEE Transactions on Microwave Theory and Techniques*, 3(10), pp.1663-1672.

Chi, P.L., 2012. Miniaturized ring coupler with arbitrary power divisions based on the composite right/left-handed transmission lines. *Microwave and Wireless Component Letters*, 22(4), pp.170-172.

Chiu, L., 2014. Wideband microstrip 90˚ hybrid coupler using high pass network. *International Journal of Microwave Science and Technology*, 2014, pp.1-6.

Dydyk, M., 1999. Microstrip directional couplers with ideal performance via single-element compensation. *IEEE Transactions on Microwave Theory and Techniques*, 47(6), pp.956-964.

Feng, W., Duan, X., Shi, Y., Zhou, X.Y., and Che, W., 2020. Dual-band branch-line couplers with short/open-ended stubs. *IEEE Transactions on Circuits and Systems II*, 67(11), pp.2497-2501.

Hong, J.S., and Lancaster, M.J., 2001. Microstrip Filters for RF/Microwave Applications. John Wiley and Sons, Hoboken.

Jia, L., Zhang, L., and Zhang, C., 2020. A dual-band and wide-band branch-line coupler with a large frequency ratio. *Microwave and Optical Technology Letters*, 63(1), pp.146-151.

Kao, C.W., and Chen, C.H., 2000. Novel uniplanar 180° hybrid-ring couplers with spiral-type phase inverters. IEEE Microwave and Guided Wave Letters, 10(10), pp.412-414.

Khan, Z.B., Mehdi, G., and Zhao, H., 2019. Design of a compact hybrid branch line coupler with 2-D implementation of stepped impedance transmission lines of high impedance ratio for wide range of harmonic suppression. *ACES Journal*, 34(8), pp.1211-1218.

Kim, C.S., Kim, Y.T., Song, S.H., Jung, W.S., Kang, K.Y., Park, J.S., and Ahn, D., 2001. A Design of Microstrip Directional Coupler for High Directivity and Tight Coupling. In: Microwave Conference. European.

Kim, C.S., Lim, J.S., Kim, D.Y., and Ahn, D., 2004. A design of single and multi-section microstrip directional coupler with the high directivity. *IEEE MTT-S International Microwave Symposium Digest*, 3, pp.1895-1898.

Kim, J.S., and Kong, K.B., 2010. Compact branch-line coupler for harmonic suppression. *Progress in Electromagnetics Research*, 16, pp.233-239.

Kumar, M., Islam, S.N., Sen, G., and Parui, S.K., 2020. Design of filtering directional coupler with improved performance. *International Journal of RF and Microwave Computer Aided Engineering*, 30(2), e22224.

Kumar, S., Tannous, C., and Danshin, T., 1995. A multisection broadband impedance transforming branch-line hybrid. *IEEE Transactions on Microwave Theory and Techniques*, 43(11), pp.2517-2523.

Lai, C.H., and Ma, T.G., 2013. Miniaturised rat-race coupler with second and third harmonic suppression using synthesised transmission lines. *Electronics Letters*, 49(22), pp.1394-1396.

Lalbakhsh, A., Mohamadpour, G., Roshani, S., Ami, M., Roshani, S., Sayem, A.S., Alibakhshikenari, M., and Koziel, S., 2021. Design of a compact planar transmission line for miniaturized rat-race coupler with harmonics suppression. *IEEE Access*, 9, pp.129207-129217.

Li, J.L., Qu, S.W., and Xue, Q., 2007. Microstrip directional coupler with flat coupling and high isolation. *Electronics Letters*, 43(4), pp.228-229.

Liou, C.Y., Wu, M.S., Yeh, J.C., Chueh, Y.Z., and Mao, S.G., 2009. A novel triple-band microstrip branch-line coupler with arbitrary operating frequencies. *IEEE Microwave and Wireless Components Letters*, 19(11), pp.683-685.

Maheswari, S., and Jayanthy, T., 2022. Design of compact branch-line coupler for Wi-max applications. *International Journal of Microwave and Optical Technology*, 17(1), pp.68-73.

March, S.L., 1982. Phase velocity compensation in parallel-coupled microstrip. *IEEE MTT-S International Microwave Symposium Digest*, 82(1), pp.410-412.

Mojarrad, S., and Basharat, H., 2015. Modified double box branch line coupler by utilizing quasi T-shape stub. *International Journal of Innovative Science Engineering and Technology*, 2(11), pp.390-393.

Nie, W., Xu, K.D., Zhou, M., Xie, L.B., and Yang, X.L., 2019. Compact narrow/wide band branch-line couplers with improved upper-stopband. *(AEÜ) International Journal of Electronics and Communications*, 98, pp.45-50.

Noori, L., and Rezaei, A., 2018. A microstrip hybrid coupler with wide stop-band using symmetric structure for wireless applications. *Journal of Microwaves Optoelectronics and Electromagnetic Applications*, 17(1), pp.23-31.

Rezaei, A., Noori, L., and Hosseini, S.M., 2018. Novel microstrip branch-line coupler with low phase shift for WLANs. *Analog Integrated Circuits and Signal Processing*, 98, pp.377-383.

Roshani, S., Yahya, S.I., Roshani, S., Farahmand, A.H., and Hemmati, S., 2022. Design of a modified compact coupler with unwanted harmonics suppression for L-band applications. *Electronics*, 11(11), 1747.

Salehi, M., and Noori, L., 2014. Novel 2.4 GHz branch-line coupler using microstrip cells. *Microwave and Optical Technology Letters*, 56(9), pp.2110-2113.

Salehi, M.R., Noori, L., and Abiri, E., 2015. Novel tunable branch-line coupler for WLAN applications. *Microwave and Optical Technology Letters*, 57(5), pp.1081-1084.

Sanna, G., Montisci, G., Jin, Z., Fanti, A., and Casula, G.A., 2018. Design of a low-cost microstrip directional coupler with high coupling for a motion detection sensor. *Electronics*, 7(2), p.25.

Santiko, A.B., Saputera, Y.P., and Wahyu, Y., 2016. Design and Implementation of Three Branch Line Coupler at 3.0 GHz Frequency for S-Band Radar System. In: The 22nd Asia-Pacific Conference on Communications. IEEE, Indonesia, pp.315-318.

Shamsinejad, S., Soleimani, M., and Komjani, N., 2008. Novel enhanced and miniaturized 90° coupler for 3G EH mixers. *Progress in Electromagnetics Research Letters*, 3, pp.43-50.

Shi, J., Qiang, J., Xu, K., Wang, Z.B., Lin, L., Chen, J.X., Liu, W., and Zhang, X.Y., 2016. A balanced filtering branch-line coupler. *IEEE Microwave and Wireless Components Letters*, 26(2), pp.119-121.

Shukor, N.A.M., and Seman, N., 2016. Enhanced design of two-section microstrip-slot branch line coupler with the overlapped k/4 open circuited lines at ports. *Wireless Personal Communications*, 88(3), pp.467-478.

Shukor, N.A.M., and Seman, N., 2020. 5G planar branch line coupler design based on the analysis of dielectric constant, loss tangent and quality factor at high frequency. *Scientific Reports*, 10, 16115.

Smolarz, R., Wincza, K., and Gruszczynski, S., 2020. Chebyshev-response branch-line couplers with enhanced bandwidth and arbitrary coupling level. *Electronics*, 9(11), 1828.

Sun, K.O., Ho, S.J., Yen, C.C., and Weide, D., 2005. A compact branch-line coupler using discontinuous microstrip lines. *IEEE Microwave and Wireless Components Letters*, 15(8), pp.519-520.

Sun, P., Chen, Q., Han, R., and Lu, A.Z., 2019. Analysis and design of wideband 90∘ microstrip hybrid coupler. *IEEE Access*, 7, pp.186409-186416.

Tang, C.W., and Chen, M.G., 2009. Design of multipassband microstrip branch-line couplers with open stubs. *IEEE Transactions on Microwave Theory and Techniques*, 57(1), pp.196-204.

Tang, C.W., Chen, M.G., Lin, Y.S., and Wu, J.W., 2006. Broadband microstrip branch-line coupler with defected ground structure. *Electronics Letters*, 42(25), pp.1458-1460.

Tang, C.W., Tseng, C.T., and Hsu, K.C., 2014. Design of wide passband microstrip branch-line couplers with multiple sections. *IEEE Transactions on Components Packaging and Manufacturing Technology*, 4(7), pp.1222-1227.

Tian, H., Chung, K.L., Liu, R., Dai, M., and Tang, W., 2019. Miniaturised quadrature hybrid coupler using composite planar transmission lines. *Electronics Letters*, 55(19), pp.1049-1051.

Tripathi, N., 2018. Review paper on microstrip directional coupler with high directivity. *International Research Journal of Engineering and Technology (IRJET)*, 5(5), pp.4149-4152.

Velan, S., and Kanagasabai, M., 2016. Compact microstrip branch-line coupler with wideband quadrature phase balance. *Microwave and Optical Technology Letters*, 58(6), pp.1369-1374.

Wang, J., Wang, B.Z., Guo, Y.X., Ong, L.C., and Xiao, S., 2007. A compact slow-wave microstrip branch-line coupler with high performance. *IEEE Microwave and Wireless Components Letters*, 17(7), pp.501-503.

Yaduvanshi, B., and Bhatia, D., 2016. Stub-Based Design of Coupled Line Directional Couplers. In: 2016 International Conference on Micro-Electronics and Telecommunication Engineering, IEEE, Ghaziabad.

Zhang, H., and Zhang, Z., 2019. Miniaturized microstrip branch-line coupler with good harmonic suppression based on radial stub loaded resonators. *Progress in Electromagnetics Research Letters*, 87, pp.15-20.